Chapter 7
Soil Acidification Patterns Under Different Geological and Climatic Conditions in Tropical Asia

Kazumichi Fujii and Arief Hartono

Abstract Tropical forests are characterized by highly weathered and acidified soils, whilst patterns and processes of soil acidification are diverse under different geological and climatic conditions. To identify the dominant processes of soil acidification in Southeast Asia, proton budgets were quantified for plant-soil systems in Indonesia and Thailand. The net proton generation by plant uptake was consistently high in the tropical forests. Acidification of soils can function as nutrient acquisition strategies of plants that promote cation mobilization through mineral weathering and cation exchange reaction. Soil solution composition indicated that organic acids are dominant anions that drive acidification in the highly acidic soils from sandy sedimentary rocks. Production of organic acids in the O horizons can be enhanced by the high activities of fungal enzymes (peroxidases) especially in the lignin-rich and P-poor litters on the highly acidic soils. On the other hand, bicarbonate also contributed to cation mobilization in the moderately acidic soils from clayey sedimentary rocks and ultramafic rocks (Indonesia) and under monsoon climate with distinct dry season (Thailand). The spatiotemporal variation in fine roots (plant uptake) and organic and carbonic acids can lead to different pathways of pedogenesis, i.e., incipient podzolization (Al eluviation/illuviation) and ferralitization (in situ weathering). The differences in acid-neutralizing capacities of parent materials and climatic patterns can generate the variability in soil acidity, and plant and microbial feedbacks can further reinforce the patterns of soil acidification.

Keywords Acid-neutralizing capacity • Dissolved organic matter • Proton budget • Soil acidity • Tropical forest

---

K. Fujii (✉)
Forestry and Forest Products Research Institute, 1 Matsunosato, Tsukuba, Ibaraki, Japan
e-mail: fkazumichi@affrc.go.jp

A. Hartono
Department of Soil Science and Land Resources, Bogor Agricultural University,
Bogor 16680, Japan

S. Funakawa (ed.), *Soils, Ecosystem Processes, and Agricultural Development*,
DOI 10.1007/978-4-431-56484-3_7

7.1 Introduction

Acidification is a common soil-forming process under humid climate where precipitation exceeds evapotranspiration (Krug and Frink 1983; Hallbäcken and Tamm 1986). In tropical regions, acidic soils (pH < 5.5) are widespread; they cover 30 % of the world's total land area and 60 % of the total area in the tropics (Sanchez and Logan 1992). The acidic soils in tropical regions generally exhibit the low concentrations of exchangeable bases, low solubility of phosphorus (P), and high concentrations of exchangeable Al and solution Al ions (Al^{3+}). These factors related to soil fertility can limit productivity of plants (esp., crop species) in tropical regions.

The decline of plant productivity has also been reported in some of tropical forests on the highly acidified and weathered soils (Vitousek and Howarth 1991). On the other hand, the massive aboveground biomass of tropical forests can be developed even on highly acidic soils in Southeast Asia (Fujii 2014). There still exist several knowledge gaps between high productivity and soil acidity.

Soil acidification induced by acidic deposition or agriculture is well known as one of soil degradation, whilst acidification is an essential process for plant nutrient acquisition. In tropical forests, the large amounts of nutrient need to be supplied from the acidic soils for plant biomass production. Basic cations (K, Mg, and Ca) and P are released from mineral dissolution and cation (or anion) exchange reactions. Most of these reactions require acidification of soil. To assess the drivers and ecological significance of soil acidification, the dominant processes of soil-acidifying processes need to be identified.

Soil acidification is caused by nitrification, the dissociation of organic acids and carbonic acid, and the excess uptake of cations over anions by plants (Van Breemen et al. 1983; Binkley and Richter 1987). Soil solution studies have revealed the roles of biologically processed anions in soil solution, i.e., organic acids, carbonic acid, and nitric acid, as drivers of cation mobilization (Ugolini and Sletten 1991). Further, theory and calculation of proton budgets in a plant-soil system can quantify contribution of external and internal proton sources to soil acidification, as it can also include proton release associated with cation uptake by plants (Van Breemen et al. 1983; Johnson 1977; Fujii et al. 2008). These studies showed that soil-acidifying processes can vary from ecosystem to ecosystem. Organic acids [dissolved organic matter (DOM)] generally play roles in acidification of the Spodosol soils in coniferous forests, while carbonic and nitric acids contribute to acidification of the Inceptisol and Andisol soils in temperate broad-leaved forests (Ugolini and Sletten 1991; Fujii et al. 2008). Calculation of proton budgets in each of soil horizon provides a better understanding of proton generation and consumption within the soil profiles.

The soil-acidifying processes can also vary between temperate and tropical forests. In several tropical forests from America, the production and leaching of carbonic acids from intensive root and microbial respiration have been reported to be a major cause of soil acidification (Johnson 1977; McDowell 1998). The hypothesis has been proposed that carbonic acid leaching has developed in tropical forests to utilize high soil CO_2 pressure to acquire exchangeable bases and to minimize leaching losses of bases from base-poor soils (Johnson 1977).

Tropical forests exhibit wide variation in vegetation, geology, and climate. Regarding specific aspects in Southeast Asia, Ashton (1988) hypothesized that Dipterocarpaceae exhibit high species diversity, tall stature, and large biomass production through adaptation to acidic soils via ectomycorrhizal associations. The high host specificity of ectomycorrhizae can cause competitive advantage and family-level monodominance of Dipterocarpaceae in Southeast Asia, whereas most of the dominant trees in America and Africa associate with vesicular-arbuscular mycorrhizae (Connell and Lowman 1989). In Southeast Asian tropical forests, nutrient acquisition of trees in the Ultisol soils may be different from those in the Oxisol and Ultisol soils of America and Africa, in that Asian Ultisol soils are richer in weatherable minerals because of steep slopes or relatively young geological ages (Fujii et al. 2011a).

We applied theory of proton budgets to individual soil horizons to identify the dominant soil-acidifying processes and the site-specific and common aspects of acidification processes in Southeast Asia by comparing with the other tropical regions.

7.2 Materials and Methods

7.2.1 Descriptions of Experimental Plots

The experimental sites include five sites from Indonesia and one site from Thailand. The sites are selected to compare effects of geology (serpentine vs mudstone vs sandstone) and climate (tropical humid vs tropical monsoon) (Table 7.1).

Five sites of tropical forests in Indonesia consisted of natural secondary forests in Kuaro (KR1, KR2, and KR3) and Bukit Soeharto (BS) and pristine forest in Bukit Bankirai (BB), East Kalimantan Province, Indonesia. The parent materials are largely sedimentary rocks, but there occur patches of serpentine (ultramafic) intrusion. The KR1, KR2, and KR3 plots are located along a traverse across serpentine-sedimentary rocks (mudstone). The KR1 soil is located on the serpentine belt and is classified as a Rhodic Eutrudox (Soil Survey Staff 2006). The KR2 soil is located in the transitional zone between serpentine and mudstone, and the KR3 soil is located on mudstone (Fig. 7.1). The KR2 and KR3 soils are classified as Typic Paleudults. The BS and BB soils are derived from sedimentary rocks (sandstone) and are classified as Typic Paleudults. The mean annual air temperature is 26.8 °C at all plots. The annual precipitation is 2256 mm $year^{-1}$ (KR1, KR2, and KR3), 2187 mm $year^{-1}$ (BS), and 2427 mm $year^{-1}$ (BB), respectively. At the KR sites, the vegetation is dominated by *Harpullia arborea* and *Bauhinia purpurea* at KR1, *Harpullia arborea* and *Durio* spp. at KR2, and *Harpullia arborea*, *Artocarpus lanceolata*, and *Durio* spp. at KR3. At the BS and BB sites, the vegetation is

Table 7.1 Description of experimental sites

Site	KR1	KR2	KR3	BS	BB	RP
Coordinates	S1°51′, E116°02′	S1°49′, E115°59′	S1°49′, E115°56′	S0°51′, E117°06′	S1°01′, E116°52′	N19°50′, E100°20′
Mean annual air temperature (°C)	27	27	27	27	27	25
Mean annual precipitation (mm)	2256	2256	2256	2187	2427	2084
Elevation (m)	92	204	167	99	80	697
Soil type[a]	Rhodic Eutrudox	Typic Paleudults	Typic Paleudults	Typic Paleudults	Typic Paleudults	Typic Haplustults
Parent material	Serpentine	Mudstone serpentine	Mudstone	Sandstone	Sandstone	Mudstone
Vegetation	*Harpullia arborea* *Bauhinia purpurea*	*Harpullia arborea Durio* spp.	*Harpullia arborea* *Artocarpus lanceolata* *Durio* spp.	*Shorea leavis* *Dipterocarpus cornutus*	*Shorea leavis* *Dipterocarpus cornutus*	*Lithocarpus* sp., *Eugenia* sp.

[a] Soils were classified according to Soil Taxonomy (Soil Survey Staff 2006)

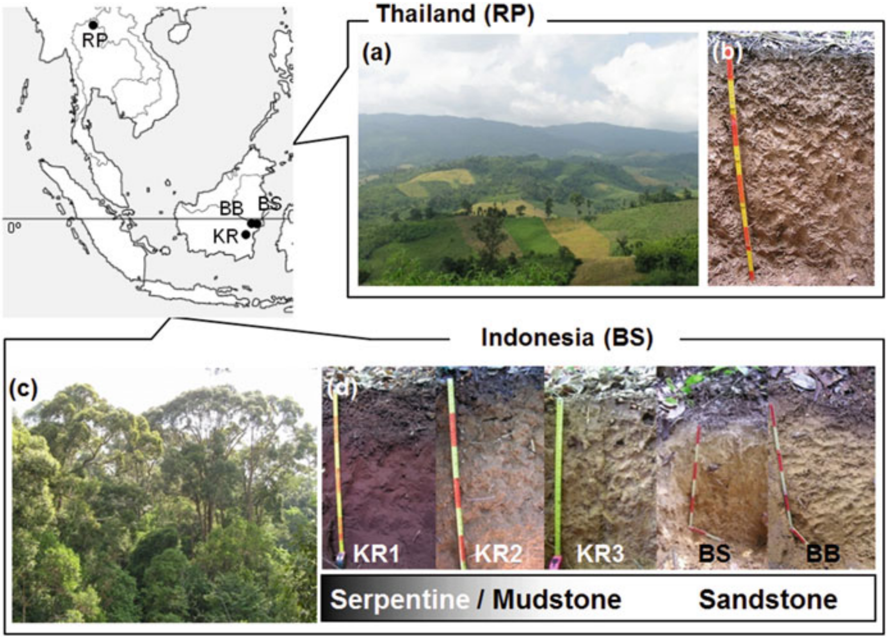

Fig. 7.1 Landscapes and soils of the experimental sites in Thailand (RP) and Indonesia (KR, BS, BB); (**a**) secondary forest/shifting cultivation landscape (RP), (**b**) Ultisol soil, (**c**) tropical lowland forest (BS), and (**d**) Oxisol and Ultisol soils in KR and Ultisol soils in BS and BB

dominated by *Shorea laevis* and *Dipterocarpus cornutus*. The detailed information of sites and soils is given in Fujii et al. (2009a, 2011c).

One site in Thailand was located in Ban Rakpaendin, Chiang Rai Province, Thailand, where the mean annual air temperature and annual precipitation are 25.0 °C and 2084 mm year^{-1}, respectively. There are distinct dry and wet seasons: the dry season is from November to March and the wet season with most of the rainfall is from April to October. Soils are derived from sedimentary rocks (mudstone) and classified as Typic Haplustults (Soil Survey Staff 2006).The vegetation is dominated by *Lithocarpus* sp. and *Eugenia* sp. in RP.

7.2.2 Soil Materials

Soil samples were air-dried and crushed to pass through a 2 mm sieve and then analyzed by the following methods. Soil pH was measured using a soil to solution (H_2O or 1 M KCl) ratio of 1:5 (w/v) after shaking for 1 h. Total carbon contents were determined using a CN analyzer (Vario Max CN, Elementar Analysensystem GmbH). Particle size distribution was determined by the pipette method. The exchangeable basic cation concentrations and CEC were determined using the ammonium acetate (1 M and pH 7.0) method. Ca and Mg in the extracts were measured using atomic absorption spectroscopy (A-A-640-01, Shimadzu), whereas Na and K were measured by flame photometry. Exchangeable Al and H were determined by titration after 1 M KCl extraction and exchangeable Al was determined using aluminon colorimetry. The contents of well and poorly crystalline Fe oxides and organic Fe compounds (Fe_d) were estimated by extraction with a citrate-bicarbonate mixed solution buffered at pH 7.3 with the addition of sodium dithionite (DCB) at 80°C (Mehra and Jackson 1960). Elemental analyses were made in hydrofluoric acid-sulfuric acid digests of soil samples (Jackson 1958). The Fe and Al contents were determined by inductively coupled plasma atomic emission spectrometry (ICP-AES, SPS1500, Seiko Instruments Inc.).

7.2.3 *Plant Materials*

Circular litter traps of 60 cm diameter were used to collect litterfall. Fine root biomass in the O horizon was estimated by collecting the roots from 30 cm × 30 cm quadrats. Fine root biomass in the mineral soil was estimated by collecting the roots in 5 cm depth intervals in cores of 0.1 L volume. Five replicates were used for all three of these measurements. Roots were rinsed in distilled water to remove soil materials. Aboveground biomass was estimated by applying the diameters of stems at breast height (DBH) to the regression equations obtained by Yamakura et al. (1986). DBH was measured by tree census. Wood increment was estimated by stem analysis (tree ring analysis) and using the regression equation for estimating tree biomass according to Johnson and Risser (1974). Wood samples were collected using an increment borer. Plant samples were oven-dried at 70°C for 48 h and then weighed and milled. The C and N concentrations in plant materials were determined using a CN analyzer. The Na and K concentrations in plant samples were determined by flame photometry, Mg and Ca concentrations by atomic absorption spectroscopy, Fe and Al contents by ICP-AES, and P concentrations colorimetrically (UV-VIS spectrophotometer UV-1200, Shimadzu) after nitric-sulfuric acid wet digestion. The Cl and S concentrations were determined by high performance liquid chromatography (HPLC, Shimadzu) after combustion according to Busman et al. (1983).

7.2.4 *Throughfall and Soil Solution*

Soil solutions were collected in five replicates using tension-free lysimeters, each draining a surface area of 200 cm^2, beneath the O (A for RP), A (BA for RP) and B (Bt1 for RP) horizons (0, 5 and 30 cm depths) at all plots. Throughfall was collected using a precipitation collector, also using five replicates. Sample solutions were filtered through 0.45 μm membrane filters before each analysis. The concentrations of H^+ in solution were determined with a glass electrode. The concentrations of Na^+, K^+, NH_4^+, Mg^{2+}, Ca^{2+}, Cl^-, NO_3^-, and SO_4^{2-} in solution were determined by HPLC. The concentrations of total Fe and Al in solution were determined by ICP-AES. The total charge equivalent of Al ions (Al^{n+}) was calculated as the equivalent sum of Al^{3+}, $AlOH^{2+}$, and $Al(OH)_2^+$. The concentrations of DOC, inorganic carbon (IC), and total dissolved N (TDN) were determined using a total organic carbon analyzer (TOC-V_{CSH}, Shimadzu). The concentrations of HCO_3^- in solution were determined from the solution pH and IC concentration, based on pKa = 6.3. The anion deficit, if any, was assigned to the negative charge of organic acids. The concentrations of dissolved organic N (DON) were calculated by subtracting NH_4^+ and NO_3^- from TDN concentrations (DON = TDN − NH_4^+ − NO_3^-).

7.2.5 Monitoring Temperature and Volumetric Water Content in Soils

The soil temperature at 5 cm depth was measured with a thermistor probe (107 Temperature Probe, Campbell Scientific, Inc.) using two replicates, while volumetric water contents in soils at depths of 5, 15, and 30 cm were measured with time domain reflectometer probes (CS615 Water Content Reflectometer, Campbell Scientific, Inc.) in three replicates. Data were recorded using data loggers at 30 min intervals (Campbell Scientific, Inc., CR-10X) during the study.

7.2.6 Ion Fluxes

Ion fluxes leached from each horizon were calculated by multiplying the water fluxes by ion concentrations in throughfall and soil solutions. Throughfall water fluxes were measured using a precipitation collector, while the half-hourly fluxes of soil water percolating at depths of 5, 15, and 30 cm were estimated by applying Darcy's law to the unsaturated hydraulic conductivity and the gradient of the hydraulic heads at each depth. The one-dimensional, vertical flow equation (Richards' equation) in the unsaturated soil zone is written as

$$C(h)\frac{\delta h}{\delta t} = \frac{\delta}{\delta z}\left[K(h)\left(\frac{\delta h}{\delta z} + 1\right)\right] - S(h) \tag{7.1}$$

where C (m^{-1}) is differential water capacity, t (day) is time, Z (m) is height, h (m) is soil water pressure head, K (m day^{-1}) is unsaturated hydraulic conductivity, and S (day^{-1}) is a sink term accounting for water uptake by vegetation and lateral water flow. The unsaturated hydraulic conductivity and soil water pressure heads at depths of 5, 15, and 30 cm were estimated using the saturated hydraulic conductivity, water retention curves of soil, and volumetric water content monitored at 30 min intervals at each depth (Mualem and Dagan 1978; Van Genuchten 1980). In this process, the Mualem-Van Genuchten parameters describing the unsaturated hydraulic conductivity and soil water pressure heads were adjusted to meet the soil water budget according to Klinge (2001). A detailed description of the calculation of soil water fluxes was given in our previous report (Fujii et al. 2008). The water fluxes for each month were calculated by summing the half-hourly water fluxes thus estimated. Ion fluxes for each month were calculated by multiplying the water fluxes by ionic concentrations in throughfall and soil solution during each month. The annual ion fluxes were each calculated by summation.

7.2.7 Proton Budgets

Net proton generation (NPG) resulting from excess cation uptake by vegetation, nitrification, dissociation of organic acids, dissociation of carbonic acid, and net proton influx from the overlying horizon can be calculated based on the input-output budget of ions in soil vegetation systems and including solute leaching and vegetation uptake (Table 7.2; Van Breemen et al. 1983, 1984). In the present study, proton budgets were quantified for each soil horizon compartment (O, A, and B horizons) using throughfall and soil solution to describe proton generation and consumption in the soil profiles (Fujii et al. 2008). Net proton generation associated with excess cation uptake by vegetation ($\mathrm{NPG_{Bio}}$), which consists of wood increment and litterfall, is calculated as

$$\mathrm{NPG_{Bio}} = (\mathrm{Cation})_{\mathrm{bio}} - (\mathrm{Anion})_{\mathrm{bio}} \tag{7.2}$$

where (Cation) and (Anion) represent the equivalent sum of cations and anions, respectively. The ionic species considered in the present study were $\mathrm{Na^+}$, $\mathrm{K^+}$, $\mathrm{Mg^{2+}}$, $\mathrm{Ca^{2+}}$, $\mathrm{Fe^{3+}}$, and $\mathrm{Al^{n+}}$ for cations and $\mathrm{Cl^-}$, $\mathrm{H_2PO_4{}^-}$, and $\mathrm{SO_4{}^{2-}}$ for anions. The suffix "bio" represents ion fluxes caused by plant uptake ($\mathrm{kmol_c\ ha^{-1}\ year^{-1}}$).

Net proton generation associated with the transformation of nitrogen ($\mathrm{NPG_{Ntr}}$) is

$$\mathrm{NPG_{Ntr}} = \left\{(\mathrm{NH_4{}^+})_{\mathrm{in}} - (\mathrm{NH_4{}^+})_{\mathrm{out}}\right\} + \left\{(\mathrm{NO_3{}^-})_{\mathrm{out}} - (\mathrm{NO_3{}^-})_{\mathrm{in}}\right\} \tag{7.3}$$

The suffix "in" represents ion fluxes percolating into the soil compartment in throughfall and the soil solution from the overlying horizon (e.g., throughfall for the O horizon), while the suffix "out" represents ion fluxes leaching out of the soil compartment in the soil solution.

Table 7.2 Representative processes of proton generation and calculation methods

H^+ budget	Representative reaction	Proton budget calculation
Proton-generating processes		
(1) H^+ input (e.g., acid rain)		H^+ input $= (H^+)_{in} - (H^+)_{out}$
(2) Cation excess uptake by plants	$Ca^{2+} + 2R{-}OH \rightarrow (R{-}O)_2Ca\ (org) + 2H^+$	$NPG_{Bio} = (Cat)_{bio} - (Ani)_{bio}$
(3) N transformation (e.g., nitrification)	$NH_4^+ + H_2O \rightarrow NO_3^- + 2H^+ + H_2O$	$NPG_{Ntr} = (NH_4^+)_{in} - (NH_4^+)_{out} + (NO_3^-)_{out} - (NO_3^-)_{in}$
(4) Dissociation of carbonic acid	$H_2CO_3 \rightarrow HCO_3^- + H^+$	$NPG_{Car} = (HCO_3^-)_{out} - (HCO_3^-)_{in}$
(5) Dissociation of organic acid	$2CH_2O + 3/2O_2 \rightarrow HC_2O_4^- + H^+ + H_2O$	$NPG_{Org} = (Org^{n-})_{out} - (Org^{n-})_{in}$
Proton-consuming processes		
(6) Weathering and cation exchange reaction	$n/2M_{2/n}O_{(s)} + nH^+ \rightarrow M^{n+} + n/2H_2O$	

The suffix "bio" represents ion fluxes ($kmol_c\ ha^{-1}\ year^{-1}$) caused by plant uptake, assuming that vegetation uptake was equal to the sum of wood increment and litterfall

The suffixes "in" and "out" represent ion fluxes entering the soil horizon (e.g., throughfall for the O horizon) and leaving the horizon, respectively

Cat and Ani represent cations (Na^+, K^+, Mg^{2+}, Ca^{2+}, Fe^{3+}, Al^{n+}) and anions (Cl^-, SO_4^{2-}, $H_2PO_4^-$), respectively

Net proton generation associated with the dissociation of organic acids (NPG_{Org}) is

$$NPG_{Org} = \left(Org^{n-}\right)_{out} - \left(Org^{n-}\right)_{in} \tag{7.4}$$

where Org^{n-} represents the negative charge of organic anions.

Net proton generation associated with carbonic acid dissociation (NPG_{Car}) is

$$NPG_{Car} = \left(HCO_3^-\right)_{out} - \left(HCO_3^-\right)_{in} \tag{7.5}$$

Net proton influx from the overlying horizon is

$$\left\{\left(H^+\right)_{in} - \left(H^+\right)_{out}\right\} \tag{7.6}$$

7.2.8 Soil Acidification Rate

Soil acidification is defined as the decrease of acid-neutralizing capacity (ANC) of the solid phase of a soil (Van Breemen et al. 1984). $ANC_{s\ (ref\ pH=3)}$ ($cmol_c\ kg^{-1}$) is conceptually defined as the sum of basic cation equivalence minus the sum of strongly acidic anion equivalence at a reference soil pH of 3. In our study, soil ANC was calculated using the equation proposed by Brahy et al. (2000):

$$
{}_{\mathrm{m}}\mathrm{ANC}_{\mathrm{s(refpH=3)}} = 2(\mathrm{Na_2O}) + 2(\mathrm{K_2O}) + 2(\mathrm{CaO}) + 2(\mathrm{MgO}) + 6(\mathrm{Fe_2O_{3tot}} - \mathrm{Fe_2O_{3d}}) + 6(\mathrm{Al_2O_3}) \quad (7.7)
$$

where parentheses denote total molar concentration. Iron-bearing silicates are considered to be ANC components, while ferric oxides are not taken into account, since at pH values above 3 they do not contribute to acid neutralization (Brahy et al. 2000). The soil acidification rate was calculated as the change in ANC components over a given period, i.e., ΔANC (kmol$_c$ ha^{-1} year^{-1}). Using ion budget in each soil horizon, the soil acidification rate (ΔANC) is

$$
\Delta\mathrm{ANC} = \left\{(\mathrm{Anion})_{\mathrm{out}} - (\mathrm{Anion})_{\mathrm{in}}\right\} - \left\{(\mathrm{Cation})_{\mathrm{out}} - (\mathrm{Cation})_{\mathrm{in}}\right\} - \left\{(\mathrm{Cation})_{\mathrm{bio}} - (\mathrm{Anion})_{\mathrm{bio}}\right\} \quad (7.8)
$$

The sum of acid load is compensated by the stoichiometric decrease of ANC. Theoretically, ΔANC, $\mathrm{NPG_{Bio}}$, $\mathrm{NPG_{Ntr}}$, $\mathrm{NPG_{Org}}$, $\mathrm{NPG_{Car}}$, and net proton influx from the overlying horizon have the following relationship:

$$
-\Delta\mathrm{ANC} = \mathrm{NPG_{Bio}} + \mathrm{NPG_{Ntr}} + \mathrm{NPG_{Org}} + \mathrm{NPG_{Car}} + \left\{(\mathrm{H^+})_{\mathrm{in}} - (\mathrm{H^+})_{\mathrm{out}}\right\}. \quad (7.9)
$$

7.3 Results

7.3.1 Physicochemical Properties of Bedrocks and Soils

The bedrocks and fresh serpentine collected in the KR1 site contained the high concentrations of Fe and Mg, while bedrocks of mudstone in the KR2, KR3, and RP sites contained the high concentrations of Al, Fe, and Si (Table 7.3). The C horizon sample of BB contains the higher concentrations of Si due to its origin of sandstone (Table 7.3).

In the BS and BB soils from sedimentary rocks (sandstone), all of the soil horizons are strongly acidic (pH 3.8–4.3), consistent with the low contents of basic cations and high Al saturation (Table 7.4). In the KR and RP soils from serpentine and sedimentary rocks (mudstone), the pH values (4.5–6.4) were higher than in the BS and BB soils (Table 7.4). Clay contents of the KR and RP soils were also higher than in the BS and BB soils (23–40 %). For Indonesian five sites, the DCB extractable Fe oxide (Fe$_d$) contents increased toward the serpentine belt and were highest in the KR1 soils from serpentine. The ANC increased with soil pH and clay content, varying from 309–643 cmol$_c$ kg^{-1} in the BS and BB soils to 1163–2012 cmol$_c$ kg^{-1} in the KR and RP soils (Table 7.4). The higher ANC values are mainly contributed by Mg and Fe in the KR1 soil and by Al in the KR2, KR3, and RP soils.

Table 7.3 Elemental composition of weathered rocks of the soil studied

	Na_2O[a]	K_2O[a]	MgO[a]	CaO[a]	Al_2O_3[a]	Fe_2O_3[a]	SiO_2[b]	P
Site	(%)							(mg kg^{-1})
Serpentine[c]	1.2	0.3	39.3	0.5	9.5	7.1	42.1	8
KR1	0.1	0.2	37.3	0.2	15.7	11.7	34.9	17
KR2	0.2	0.3	8.8	0.1	11.8	8.5	70.3	700
KR3	0.1	0.9	0.1	0.1	9.3	6.4	83.2	172
BB[d]	0.1	1.3	0.2	0.0	4.9	3.4	90.1	98
RP	0.3	4.4	0.0	0.0	21.8	8.8	64.6	281

[a] Oven-dried basis. Elemental analyses were made in hydrofluoric-sulfuric acid digestion

[b] $(SiO_2\%) = 100\ \% - \{(Na_2O\ \%) + (K_2O\ \%) + (MgO\ \%) + (CaO\ \%) + (Fe_2O_3\%) + (Al_2O_3\%)\}$

[c] Fresh serpentine rock sample collected from the bedrock outcrop close to KR1

[d] Rock sample could not be available. The data of the C horizon were presented for BB

The O horizons had only an Oi layer in the KR1, KR2, and RP soils, while they consisted of an Oea layer, as well as a Oi layer, in the acidic BS, BB, and KR3 soils ($pH < 4.5$) (Table 7.5). In the BB and BS soils, the O horizons are acidic (pH 4.5 to 5.0), consistent with lower concentrations of basic cations (17–63 $cmol_c\ kg^{-1}$). The higher concentrations of basic cations in the O horizons of the KR and RP soils (87–129 $cmol_c\ kg^{-1}$) are probably a consequence of parent materials rich in basic cations (Tables 7.3 and 7.5).

7.3.2 C Stock and Flow in Soils and Ecosystems

In five sites in Indonesia, the aboveground biomass (259.8 to 346.0 Mg C ha^{-1}) was greater than in RP, with the considerably lower exception of KR1 (134.2 Mg C ha^{-1}; Fig. 7.2). The fine root biomass was mainly distributed in the mineral soil horizons of all plots; however, it was also distributed in the O horizons of the KR3, BS, and BB soils (Fig. 7.3; 0.3–2.3 Mg C ha^{-1}). The C stock in the organic and mineral soil horizons is 2.9–4.1 and 26.6–74.7 Mg C ha^{-1}, respectively. The higher aboveground biomass and low C stock in the organic and mineral soil horizons in our study, as compared to temperate forests, are consistent with a previous report (Nakane 1980).

The rates of litterfall and wood increment in our study (3.6–4.8 and 5.1–11.1 Mg C ha^{-1}, respectively) are also higher than in temperate forests, owing to the higher primary production in tropical regions (Table 7.6).

7.3.3 Soil Solution Composition and Ion Fluxes in Throughfall and Soil Solution

Soil solution composition and ion fluxes are presented in Tables 7.7 and 7.8 (or Fig. 7.4), respectively. Soil solutions were strongly acidic in the BS and BB

Table 7.4 Physicochemical properties of the forest soils in Indonesia and Thailand

Site	Horizon	Depth (cm)	pH		Total	Total	CN ratio	CEC^a	Exchangeable cation[a]			Particle size distribution[ac]			$Fe_d{}^a$	Total content[a]					Fe_2O_3	$_mANC_{(s)}{}^{ad}$	Base[ae]
			H_2O	KCl	C^a	N^a			Base[b]	Al	H	Sand	Silt	Clay		Na_2O	K_2O	MgO	CaO	Al_2O_3			
					$(g\ kg^{-1})$				$(cmol_c\ kg^{-1})$			(%)			$(g\ kg^{-1})$	(%)						$(cmol_c\ kg^{-1})$	
KR1	A1	0–5	6.3	5.8	72.7	6.4	11	24.8	19.1	0.0	1.1	6	39	55	176	0.1	0.1	1.3	0.2	4.7	51.8	1358	80
	A2	5–20	6.2	5.7	23.8	2.6	9	11.4	5.0	0.0	1.1	14	45	41	196	0.2	0.1	1.2	0.0	5.8	60.0	1608	71
	B1	20–35	6.4	6.1	7.5	0.8	9	7.2	2.0	0.0	0.9	19	37	44	208	0.0	0.1	1.1	0.0	6.1	67.2	1817	57
	B2	35–50	6.4	5.8	5.7	0.7	8	7.0	1.8	0.0	0.7	16	37	47	217	0.1	0.1	1.2	0.0	6.3	68.7	1853	68
	B3	50–67+	6.4	6.2	4.8	0.6	8	7.7	2.7	0.0	0.8	38	33	28	216	0.1	0.1	0.9	0.0	6.2	65.7	1725	53
KR2	A	0–5	5.6	5.2	73.1	5.5	13	19.8	14.5	0.2	1.2	6	15	79	67	0.0	0.3	0.5	0.2	28.2	13.2	1837	39
	BA	5–20	4.6	3.9	24.9	2.9	9	13.7	1.4	2.9	2.4	5	18	77	71	0.2	0.3	0.3	0.0	31.3	14.0	2012	30
	Bt1	20–45	4.8	4.1	14.2	1.8	8	17.0	1.0	2.3	1.4	4	10	86	71	0.0	0.3	0.3	0.0	31.6	13.7	2011	23
	Bt2	45–70+	5.1	4.2	10.0	1.4	7	24.8	0.8	1.4	1.5	7	11	82	78	0.1	0.3	0.3	0.0	32.2	13.2	1996	25
KR3	A	0–4	4.5	3.7	38.7	3.5	11	20.8	1.8	4.9	2.8	28	24	48	30	0.1	0.2	0.4	0.2	17.6	6.8	1163	33
	BA	4–15	4.5	3.7	17.9	1.7	10	17.2	1.0	4.9	1.9	29	15	56	32	0.1	0.2	0.4	0.0	19.2	6.9	1245	30
	Bt1	15–30	4.5	3.7	11.1	1.2	9	19.7	1.2	6.3	1.5	28	15	57	34	0.0	0.2	0.4	0.0	20.0	7.2	1293	27
	Bt2	30–45	4.6	3.8	7.4	0.9	9	23.3	1.4	7.0	1.0	25	15	60	36	0.1	0.3	0.4	0.0	22.2	7.7	1430	30
	Bt3	45–50+	4.6	3.8	7.5	1.0	8	27.1	0.9	7.7	0.5	25	9	66	38	0.1	0.2	0.4	0.0	22.6	8.0	1459	30
BS	A	0–5	4.0	3.9	22.9	1.6	14	8.5	2.2	3.0	5.7	52	25	23	7	0.1	0.4	0.2	0.1	4.1	2.1	309	26
	BA	5–25	3.8	3.8	4.2	0.5	9	6.2	0.8	3.9	6.1	49	27	24	9	0.3	0.5	0.2	0.1	5.7	2.4	413	33
	B1	25–40	4.0	3.8	3.5	0.5	7	5.0	0.8	4.8	6.5	43	30	27	11	0.3	0.5	0.3	0.1	7.3	2.7	502	36
	Bt	40–50+	4.3	3.8	2.5	0.4	6	5.0	1.0	7.0	7.7	34	35	31	15	0.2	0.7	0.3	0.0	9.4	3.6	643	35

BB	A	0–5	4.2	3.4	36.1	2.3	16	13.0	1.2	6.7	8.5	42	31	27	9	0.2	0.6	0.2	0.1	4.9	3.4	400	32
	BA	5–20	4.1	3.7	10.7	0.9	13	8.3	0.8	5.5	7.2	45	31	24	11	0.2	0.4	0.2	0.1	5.8	1.5	369	30
	B1	20–37	4.1	3.8	7.1	0.6	11	8.5	1.1	5.7	8.2	43	33	24	11	0.2	0.5	0.3	0.1	6.7	2.1	440	32
	Bt	37–70	4.1	3.8	3.7	0.4	8	9.0	0.8	4.6	7.3	39	34	27	15	0.3	0.6	0.3	0.1	8.1	2.7	531	37
	BC	70+	4.2	3.8	3.3	0.4	8	13.6	0.9	6.7	7.5	34	25	40	18	0.1	0.6	0.3	0.0	9.4	3.9	630	28
RP	A	0–7	5.0	4.1	62.6	3.8	17	27.6	5.8	0.8	1.5	5	25	70	33	0.2	3.4	1.1	0.1	18.7	6.9	1324	139
	BA	7–20	4.9	3.9	19.8	1.5	13	19.9	2.0	1.5	1.6	4	23	73	36	0.3	3.8	1.3	0.0	23.1	8.1	1627	157
	Bt	20–45+	4.6	4.0	8.9	1.0	9	20.1	1.4	1.5	1.6	6	19	75	43	0.4	3.9	1.2	0.0	24.7	9.0	1716	158

[a] Oven-dried basis

[b] Na^++K^++Mg^{2+}+Ca^{2+}

[c] Clay (<0.002 mm), silt (0.002–0.05 mm), sand (0.05–2 mm)

[d] $2(Na_2O) + 2(K_2O) + 2(MgO) + 2(CaO) + 6(Fe_2O_{3tot}{-}Fe_2O_{3d}) + 6(Al_2O_3)$

[e] $2(Na_2O) + 2(K_2O) + 2(MgO) + 2(CaO)$

Table 7.5 Physicochemical properties of the O horizons in Indonesia and Thailand

		Mass		C	N		Lignin	Na[b]	K[b]	Mg[b]	Ca[b]	Basic cation
Site	Horizon	(Mg ha^{-1})	pH[a]	(%)		C/N	(%)	(g kg^{-1})				($cmol_c$ kg^{-1})
KR1	Oi	8.2	6.5	43.5	1.1	38	35.0	0.5	5.6	2.3	7.2	87
KR2	Oi	7.8	7.4	47.1	1.5	32	28.0	0.4	4.3	4.7	11.3	129
KR3	Oi	4.0	5.9	44.0	1.1	41	42.0	0.5	5.2	3.7	9.0	108
	Oea	5.0	5.3	34.9	1.4	26	42.0	1.2	2.7	4.4	6.6	88
BS	Oi	6.0	5.0	49.3	1.2	41	44.0	0.4	5.5	2.3	4.4	63
	Oea	5.3	4.5	28.9	1.2	24	43.0	0.9	2.0	0.9	1.5	25
BB	Oi	4.5	5.0	53.2	1.4	39	46.0	0.7	3.2	2.4	1.5	35
	Oea	4.0	4.6	27.5	1.1	25	36.0	0.5	2.1	0.8	0.7	17
RP	Oi	6.0	5.9	43.1	0.7	61	24.0	0.7	5.7	4.6	10.0	123

[a] The pH was measured using the milled litter to solution (water) ratio of 1:20 for 1 h

[b] The cation concentrations were determined after nitric-sulfuric acid wet digestion

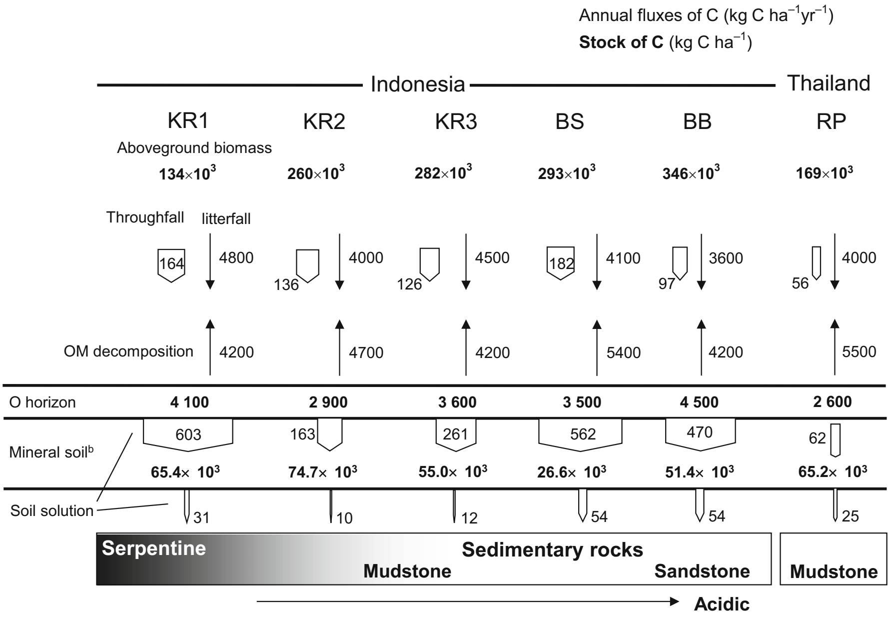

Fig. 7.2 Stocks and fluxes of C in tropical forest ecosystems. *Blank arrows* indicate DOC fluxes within ecosystems

Fig. 7.3 Depth distribution of fine root biomass in the tropical forest soils. *Bars* indicate standard errors ($n = 5$)

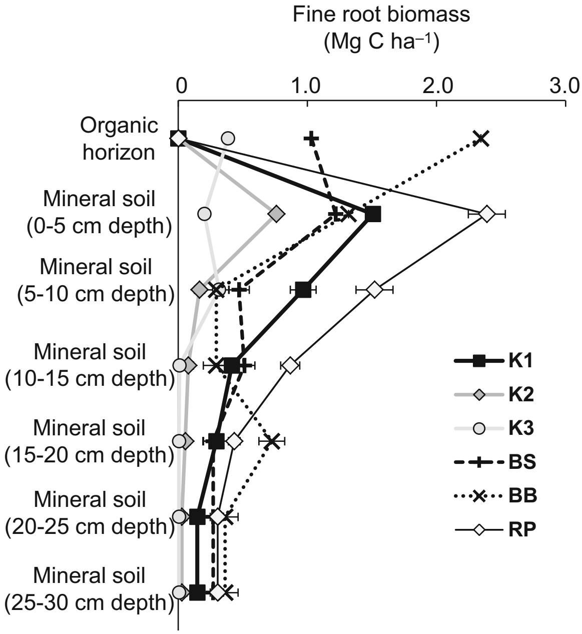

Table 7.6 Uptake of cations and anions by plants

Site		OM[a] production	Na	K	Ca	Mg	Fe	Al	Cl	S	P	Σcation	Σanion	NPG_{Bio}
		(Mg C ha^{-1} year^{-1})	(kg ha^{-1} year^{-1})									(kmol$_c$ ha^{-1} year^{-1})		
Indonesia														
KR1	Wood increment	7.2	3	53	59	9	2	1	4	4	6	5.3	0.5	4.8
	Litterfall	5.7	5	64	82	26	0	2	1	8	4	8.4	0.6	7.7
KR2	Wood increment	9.8	3	55	133	10	0	1	2	5	5	9.1	0.6	8.6
	Litterfall	3.6	3	31	81	34	1	19	1	9	5	9.9	0.7	9.1
KR3	Wood increment	5.1	3	23	42	3	1	2	1	3	2	3.3	0.3	3.0
	Litterfall	4.5	5	27	57	33	2	2	1	8	4	6.8	0.7	6.1
BS	Wood increment	10.6	15	33	29	16	10	1	1	9	2	4.7	0.6	4.0
	Litterfall	4.1	4	45	36	19	2	3	1	5	3	5.0	0.4	4.6
BB	Wood increment	11.1	15	35	31	17	2	5	1	9	2	5.1	0.7	4.5
	Litterfall	3.6	5	23	15	17	2	4	1	5	3	3.5	0.5	3.1
Thailand														
RP	Wood increment	5.8	9	21	9	3	4	4	1	0	1	2.1	0.1	2.1
	Litterfall	3.4	3	23	41	19	1	1	1	2	2	3.9	0.4	3.5

[a] OM represents organic matter

soils (pH 3.9–4.4), while they were moderately acidic at the KR and RP soils (pH 5.0–6.2) (Table 7.7). The concentrations and fluxes of DOC in the O horizon were higher in the BS, BB, and KR1 soils compared to the KR2 and KR3 soils (Table 7.7; Fig. 7.2). The DOC concentrations were low throughout the soil profile of RP. Organic acids were the dominant anions in the O horizon solution in all plots except for the KR2 and RP soils (Table 7.7). The concentrations of organic acids and DOC in the soil solution decreased with depth (Table 7.7). From linear regression analysis between the concentrations of DOC and organic acids in soil solutions, the negative charge per 1 mole of DOC (0.09–0.17 mol_c) corresponds to one dissociated acidic functional group for 5.9–11.5 C atoms. The high ratios of DOC to charge in the soil solution suggest the presence of high molecular weight fulvic acids, which contain 7 C atoms for each acidic functional group (Thurman 1985).

Bicarbonate is present in moderately acidic soil solutions of the KR and RP sites, while it was negligible in acidic soil solutions of the BS and BB sites (Table 7.6). In the O horizon of the KR2 soil, bicarbonate was the dominant anion owing to the relatively high solution pH, while concentrations decreased with depth (Table 7.7).

Nitrogen in soil solution was dominated by nitrate in KR1, KR2, and RP soils, while DON and NH_4^+ also accounted for considerable fraction of TDN (Fig. 7.5). Nitrate concentrations were low (0.02–0.16 $\text{mmol}_c\ L^{-1}$) at all plots except for the A1 and A2 horizons of the KR1 soil (Table 7.7; 0.31–0.47 $\text{mmol}_c\ L^{-1}$), where the understory vegetation was the nitrogen-fixing *Bauhinia purpurea*. The major accompanying cations were K^+, Mg^{2+}, and Ca^{2+} in the KR1, KR2, and KR3 soils, while they were H^+, NH_4^+, and Al^{n+}, as well as basic cations, in the BS and BB soils (Table 7.7). The Si concentrations in the soil solution were highest in KR1 (0.14–-0.63 mmol L^{-1}) compared to the other soils from sedimentary rocks (Table 7.7; 0.02–0.07 mmol L^{-1}).

7.3.4 Proton Budgets in Soils

Cation concentrations exceeded anion concentrations in litter and wood materials at all plots (Table 7.6). Excess cation charge was compensated for by the net proton load to the soil as NPG_{Bio}. NPG_{Bio} in each of the soil horizons was calculated by distributing it based on the distribution of the fine root biomass in the soil profiles (Fig. 7.3), according to Shibata et al. (1998). Based on the fluxes of solutes entering and leaving the soil horizon compartment (Table 7.8; Fig. 7.4) and plant uptake (Table 7.6; NPG_{Bio}) in each of the soil horizons, net proton generation and soil acidification rates were calculated based on proton budget theory. The example in the BS soils was shown in Fig. 7.6.

In the entire soil profiles, NPG_{Bio} was highest among the proton sources at all plots (Fig. 7.7). NPG_{Bio} was present mainly in the A and B horizons of soils at all plots (1.7–10.8 $\text{kmol}_c\ \text{ha}^{-1}\ \text{year}^{-1}$), while it was also present in the O horizons of the KR3, BS, and BB soils (Fig. 7.7; 1.5–3.1 $\text{kmol}_c\ \text{ha}^{-1}\ \text{year}^{-1}$). In the O horizons, proton

Table 7.7 Annual volume-weighed mean concentrations of ions in throughfall and soil solution

			DOC	IC	HCO_3^-	Cl^-	NO_3^-	SO_4^{2-}	Org^{n-b}	H^+	Na^+	NH_4^+	K^+	Mg^{2+}	Ca^{2+}	Fe^{2+}	Al^{n+c}	Si
Site	Horizon	pH	(mg C L^{-1})		(mmol$_c$ L^{-1})													(mmol L^{-1})
Indonesia																		
KR1	TF[a]	6.3	7.3	1.1	0.05	0.05	0.02	0.02	0.14	0.00	0.02	0.02	0.07	0.08	0.08	0.00	0.00	0.02
	O	6.1	31.6	2.0	0.08	0.17	0.10	0.06	0.27	0.00	0.04	0.03	0.20	0.21	0.20	0.00	0.00	0.14
	A1	5.7	13.4	0.8	0.03	0.09	0.47	0.08	0.16	0.00	0.03	0.04	0.15	0.38	0.21	0.00	0.00	0.27
	A2	6.2	5.4	4.3	0.16	0.10	0.24	0.07	0.15	0.00	0.04	0.04	0.07	0.38	0.23	0.00	0.00	0.63
KR2	TF[a]	6.2	6.2	1.3	0.05	0.02	0.03	0.05	0.07	0.00	0.02	0.01	0.05	0.06	0.08	0.00	0.00	0.02
	O	6.5	8.6	3.4	0.18	0.04	0.09	0.08	0.12	0.00	0.02	0.02	0.09	0.15	0.21	0.00	0.01	0.02
	A	5.9	5.7	0.7	0.03	0.02	0.07	0.02	0.05	0.00	0.01	0.01	0.02	0.06	0.07	0.00	0.01	0.05
	BA, Bt	5.1	1.7	0.2	0.00	0.01	0.06	0.03	0.03	0.01	0.02	0.01	0.01	0.03	0.03	0.00	0.01	0.07
KR3	TF[a]	6.1	5.7	1.1	0.04	0.03	0.01	0.03	0.07	0.00	0.02	0.01	0.03	0.05	0.07	0.00	0.00	0.02
	O	5.6	16.4	1.3	0.04	0.08	0.03	0.06	0.22	0.00	0.02	0.02	0.08	0.15	0.13	0.00	0.02	0.08
	A	5.0	10.1	0.4	0.01	0.06	0.06	0.04	0.18	0.01	0.02	0.03	0.06	0.12	0.08	0.00	0.02	0.05
	BA, Bt1	5.1	2.8	0.1	0.00	0.03	0.02	0.01	0.04	0.01	0.01	0.01	0.02	0.03	0.01	0.00	0.01	0.03

BS	TF[a]	5.2	9.0	0.4	0.01	0.04	0.04	0.06	0.10	0.01	0.03	0.04	0.08	0.05	0.04	0.00	0.01	0.02
	O	4.4	34.7	0.2	0.00	0.06	0.04	0.07	0.26	0.04	0.04	0.09	0.11	0.07	0.04	0.02	0.04	0.07
	A	4.2	17.2	0.1	0.00	0.05	0.04	0.05	0.20	0.06	0.04	0.04	0.07	0.05	0.03	0.01	0.04	0.07
	BA, B1	4.4	9.9	0.1	0.00	0.06	0.03	0.06	0.12	0.04	0.04	0.02	0.06	0.04	0.04	0.00	0.03	0.05
BB	TF[a]	5.5	4.7	0.2	0.00	0.07	0.02	0.03	0.09	0.00	0.04	0.03	0.07	0.03	0.03	0.00	0.00	0.01
	O	4.1	24.6	0.1	0.00	0.12	0.14	0.05	0.26	0.12	0.04	0.11	0.12	0.08	0.04	0.02	0.05	0.07
	A	4.0	19.1	0.1	0.00	0.10	0.16	0.06	0.21	0.13	0.04	0.06	0.11	0.08	0.04	0.01	0.07	0.07
	BA, B1	4.1	6.0	0.1	0.00	0.11	0.10	0.06	0.13	0.09	0.05	0.03	0.09	0.05	0.03	0.01	0.06	0.07
Thailand																		
RP	TF[a]	6.1	2.7	0.5	0.02	0.01	0.01	0.01	0.02	0.00	0.01	0.01	0.00	0.01	0.02	0.00	0.00	0.00
	A	6.2	3.9	0.7	0.04	0.04	0.14	0.05	0.13	0.00	0.03	0.02	0.05	0.08	0.14	0.01	0.05	0.06
	BA	6.1	3.1	0.7	0.05	0.04	0.14	0.05	0.09	0.00	0.04	0.02	0.04	0.06	0.15	0.01	0.03	0.05
	Bt	6.1	3.1	1.1	0.04	0.04	0.06	0.05	0.04	0.01	0.04	0.02	0.03	0.03	0.08	0.01	0.02	0.06

[a] TF represents throughfall

[b] Org^{n-} represents anion deficit, the negative charge of organic acids

[c] The total charge equivalent of Al ions was calculated as the equivalent sum of Al^{3+}, $AlOH^{2+}$, and $Al(OH)_2^+$

Table 7.8 Annual fluxes of solutes in throughfall and soil solution of Thailand and Indonesia

		H_2O	DOC	IC	DON	DIN								H^+	Na^+									Si
Site	Horizon	(mm $year^{-1}$)	(kg C ha^{-1} $year^{-1}$)		(kg N ha^{-1} $year^{-1}$)		DON /TDN	DOC /DON	HCO_3^-	Cl^-	NO_3^-	SO_4^{2-}	Org^{n-b}	$kmol_c$ ha^{-1} $year^{-1}$		NH_4^+	K^+	Mg^{2+}	Ca^{2+}	Fe^{2+}	Al^{n+c}	Σcation	Σanion	(kmol ha^{-1} $year^{-1}$)
Indonesia																								
KR1	TF[a]	2240	164	24	15	12	56	11	1.05	1.12	0.45	0.38	3.19	0.01	0.51	0.38	1.56	1.83	1.86	0.01	0.04	6.19	6.19	0.34
	O	1907	603	38	21	34	39	29	1.56	3.32	1.86	1.07	5.19	0.01	0.82	0.53	3.74	3.93	3.77	0.08	0.06	14.22	13.00	2.67
	A1	1071	144	8	5	76	6	28	0.32	0.95	4.99	0.86	1.77	0.02	0.34	0.45	1.63	4.02	2.26	0.01	0.04	8.77	8.89	2.95
	A2	566	31	24	1	22	5	26	0.91	0.55	1.34	0.38	0.87	0.00	0.24	0.23	0.41	2.15	1.29	0.00	0.00	4.59	4.05	5.12
KR2	TF[a]	2211	136	28	4	12	27	31	1.06	0.52	0.59	1.00	1.55	0.01	0.42	0.27	1.05	1.25	1.66	0.01	0.06	4.73	4.72	0.40
	O	1922	166	66	4	29	13	39	3.52	0.71	1.74	1.46	2.31	0.01	0.37	0.32	1.75	2.94	3.98	0.01	0.11	9.49	9.74	0.41
	A	967	55	7	2	11	14	30	0.25	0.15	0.69	0.24	0.52	0.01	0.14	0.08	0.16	0.61	0.70	0.03	0.08	1.82	1.85	0.44
	BA, Bt	553	10	1	1	6	11	14	0.01	0.06	0.34	0.16	0.16	0.04	0.10	0.06	0.08	0.18	0.18	0.01	0.04	0.69	0.73	0.36
KR3	TF[a]	2205	126	24	6	8	41	23	0.80	0.67	0.28	0.66	1.65	0.02	0.37	0.28	0.68	1.03	1.62	0.00	0.04	4.05	4.05	0.34
	O	1594	261	20	7	11	39	36	0.62	1.27	0.55	0.88	3.45	0.04	0.32	0.27	1.34	2.36	2.11	0.07	0.25	6.77	6.78	1.20
	A	645	65	3	3	8	24	25	0.06	0.38	0.39	0.26	1.16	0.07	0.14	0.21	0.40	0.75	0.54	0.02	0.10	2.23	2.26	0.35
	BA, Bt1	416	12	0	1	2	32	16	0.00	0.11	0.08	0.06	0.15	0.03	0.04	0.03	0.07	0.11	0.06	0.01	0.04	0.39	0.39	0.11

BS	TF[a]	2031	182	9	15	21	42	12	0.18	0.81	0.72	1.30	2.06	0.12	0.67	0.77	1.57	0.94	0.81	0.06	0.14	5.07	5.08	0.34
	O	1619	562	3	19	29	40	30	0.02	1.02	0.61	1.18	4.16	0.59	0.66	1.43	1.72	1.14	0.62	0.30	0.64	7.11	6.99	1.03
	A	1196	206	2	9	13	40	23	0.00	0.54	0.52	0.65	2.34	0.73	0.47	0.42	0.87	0.66	0.35	0.11	0.46	4.07	4.06	0.77
	BA, B1	545	54	1	4	4	49	15	0.02	0.33	0.17	0.30	0.65	0.22	0.21	0.10	0.32	0.23	0.20	0.03	0.15	1.46	1.47	0.32
BB	TF[a]	2068	97	4	5	15	23	21	0.07	1.43	0.49	0.60	1.77	0.10	0.80	0.62	1.39	0.68	0.66	0.03	0.08	4.36	4.37	0.17
	O	1914	470	2	11	65	15	42	0.00	2.27	2.63	1.05	4.99	2.25	0.83	2.03	2.22	1.51	0.84	0.30	1.02	10.89	10.95	1.33
	A	1639	313	1	8	50	14	39	0.01	1.66	2.64	0.98	3.46	2.14	0.61	0.93	1.88	1.26	0.66	0.21	1.09	8.75	8.75	1.23
	BA, B1	893	54	1	2	17	10	28	0.00	1.00	0.92	0.52	1.18	0.78	0.41	0.27	0.77	0.48	0.30	0.08	0.55	3.62	3.62	0.64
Thailand																								
RP	TF[a]	2083	56	11	3	9	29	17	0.60	0.94	0.36	0.26	0.31	0.02	0.15	0.25	0.81	0.59	0.62	0.00	0.03	2.47	2.47	0.05
	A	1602	62	11	3	6	32	21	0.54	0.90	0.33	0.26	0.31	0.01	0.30	0.11	0.74	0.49	0.45	0.11	0.14	2.34	2.35	0.97
	BA	1162	36	8	2	5	29	17	0.34	0.55	0.29	0.14	0.14	0.01	0.19	0.08	0.43	0.34	0.24	0.07	0.09	1.45	1.47	0.62
	Bt	825	25	9	2	3	43	11	0.24	0.46	0.15	0.11	0.10	0.01	0.20	0.06	0.31	0.21	0.16	0.06	0.03	1.05	1.06	0.50

[a] TF represents throughfall. DIN represents sum of NH_4^+ and NO_3^-

[b] Org^{n-} represents anion deficit, the negative charge of organic acids

[c] The total charge equivalent of Al ions was calculated as the equivalent sum of Al^{3+}, $AlOH^{2+}$, and $Al(OH)_2^+$

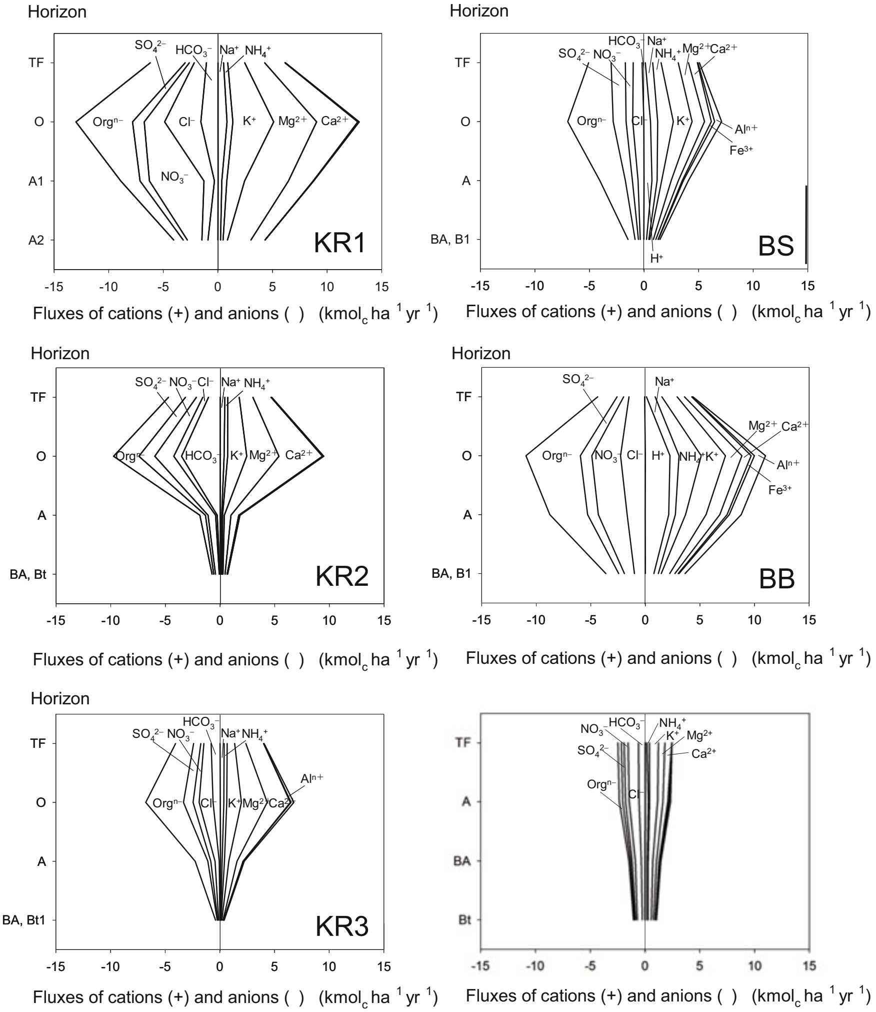

Fig. 7.4 Annual fluxes of cations and anions at each horizon. TF represents throughfall. O, A, A1, A2, BA, B1, Bt1, and Bt represent soil horizons

sources include NPG_{Org}, NPG_{Car}, and NPG_{Ntr}, as well as NPG_{Bio} (Fig. 7.7). NPG_{Org} is the largest proton source in the O horizons (NPG_{Org}, 1.8–3.2 $kmol_c$ ha^{-1} $year^{-1}$) except for the KR2 soil, where NPG_{Car} is higher than NPG_{Org} (0.8 $kmol_c$ ha^{-1} $year^{-1}$). In the moderately acidic O horizons of the KR1 and KR2 soils, protons were produced by the dissociation of carbonic acid (Fig. 7.7; NPG_{Car}, 0.5–2.5 $kmol_c$ ha^{-1} $year^{-1}$). In the A and B horizons, protons were consumed by mineralization and adsorption of organic acids and by protonation of carbonic acid (Fig. 7.7). In the RP soil, NPG_{Bio} was the dominant proton source, while NPG_{Org}, NPG_{Car}, and NPG_{Ntr} were small throughout the soil profile.

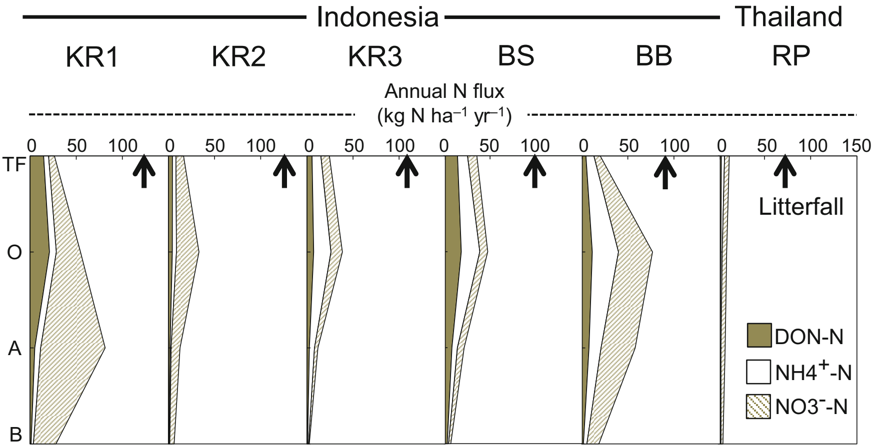

Fig. 7.5 Fluxes of N in litterfall, throughfall, and soil solution of tropical forest ecosystems. *Blank arrows* indicate litterfall N flux within ecosystems. TF, O, A, and B represent throughfall and O, A, and B horizons

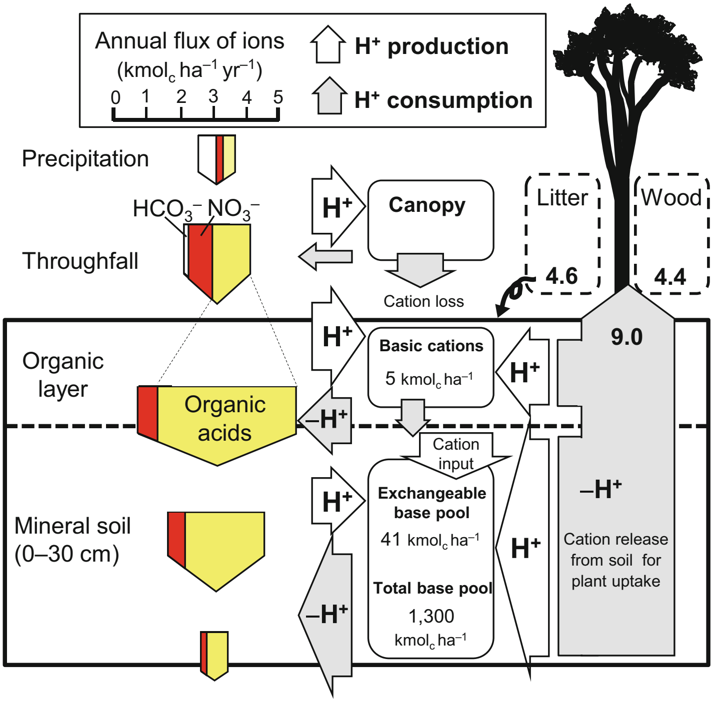

Fig. 7.6 Generation and consumption of protons in soil of the BS (Bukit Soeharto) in East Kalimantan, Indonesia. The *white arrows* indicate proton generation, whereas the *shaded arrows* indicate proton consumption (Data sources are Fujii et al. (2009a, 2010a))

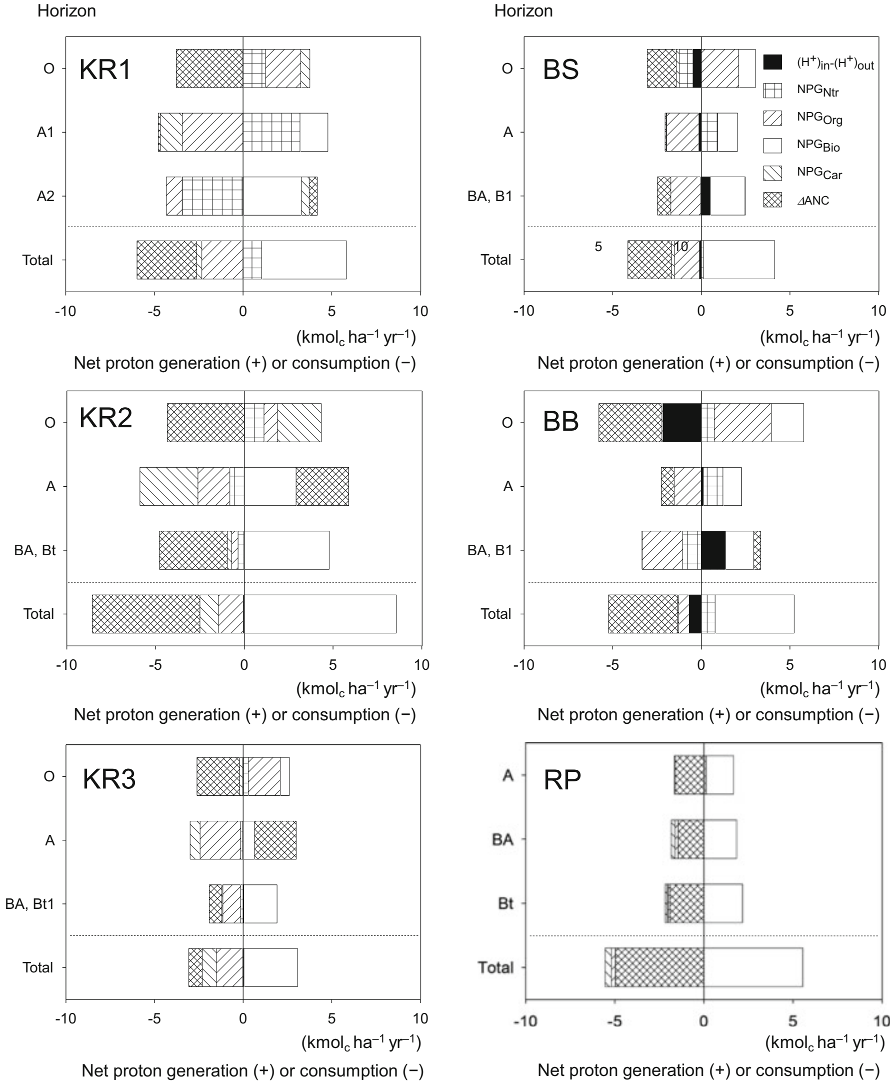

Fig. 7.7 Net proton generation and consumption in the soil profiles. TF represents throughfall. O, A, A1, A2, BA, B1, Bt1, and Bt represent soil horizons

Protons were produced by nitrification in the O horizons of the KR1, KR2, KR3, and BB soils (NPG_{Ntr}, 0.3–1.3 $kmol_c$ ha^{-1} $year^{-1}$), while they were consumed by nitrate uptake by vegetation or microorganisms in the A and B horizons. The low NPG_{Ntr} in the RP soil indicated that proton generation due to nitrification appeared to be immediately compensated by nitrate uptake by plants in the same horizon. In the acidic O horizons of the BS and BB soils, an increase in the NH_4^+ flux (Fig. 7.2;

0.6 $\text{kmol}_c\ \text{ha}^{-1}\ \text{year}^{-1}$) indicated that protons were mainly consumed by mineralization of organic N to NH_4^+ (Fig. 7.7; NPG_{Ntr}, −0.7 $\text{kmol}_c\ \text{ha}^{-1}\ \text{year}^{-1}$). In the A horizons of the BS and BB soils, protons were released owing to the excess uptake of NH_4^+ over NO_3^- by biomass or adsorption of NH_4^+ on clays (Fig. 7.7; NPG_{Ntr}, 0.9–1.1 $\text{kmol}_c\ \text{ha}^{-1}\ \text{year}^{-1}$). Exceptionally, in the A1 horizon of the KR1 soil, where understory vegetation was the nitrogen-fixing *Bauhinia purpurea*, protons were produced by nitrification (Table 7.4; NPG_{Ntr}, 3.2 $\text{kmol}_c\ \text{ha}^{-1}\ \text{year}^{-1}$).

In the O horizons of the KR soils, acid load contributed mainly by NPG_{Ntr}, NPG_{Org}, and NPG_{Car} (3.5–4.3 $\text{kmol}_c\ \text{ha}^{-1}\ \text{year}^{-1}$) was completely neutralized by basic cations (Fig. 7.8). On the other hand, in the O horizons of BS and BB, the intensive acid load contributed mainly by NPG_{Org} and NPG_{Bio} (3.2–7.0 $\text{kmol}_c\ \text{ha}^{-1}\ \text{year}^{-1}$) was largely neutralized by basic cations, but a portion of protons were transported downward. The protons transported from the O horizon ($(H^+)_{in}$-$(H^+)_{out}$, 0.5–1.4 $\text{kmol}_c\ \text{ha}^{-1}\ \text{year}^{-1}$) are neutralized in the B horizons of the BS and BB soils or are leached further downward (Figs. 7.7 and 7.8).

Using the bulk density and exchangeable acidity, the amounts of acidity accumulated in the soils in the form of exchangeable acidity were estimated to be 23–570 $\text{kmol}_c\ \text{ha}^{-1}\ \text{year}^{-1}$. When we compare the sizes of exchangeable acidity in the soils and cumulative NPG needed for cation uptake for production of standing wood biomass (Fig. 7.9), the exchangeable acidity is greater than NPG attributable to wood production in the soils except for the KR1 and KR2 soils.

7.4 Discussion

7.4.1 Dominant Soil Acidification Processes in Tropical Forests

Proton budget theory allows us to quantify contribution of proton sources including plant uptake to soil acidification. In the tropical forests studied, NPG_{Bio} is a dominant proton source in the whole soil profiles (Fig. 7.7). The soil acidification rates of tropical forests are higher than those of temperate forests [0.1–4.6 $\text{kmol}_c\ \text{ha}^{-1}\ \text{year}^{-1}$ from Bredemeier et al. (1990); Binkley (1992); Shibata et al. (2001), and Fujii et al. (2008)]. The higher acid load in tropical regions is considered to be caused by higher biomass production and resulting higher demand of basic cations (Table 7.6). Since NPG_{Bio} attributable to litter production would be neutralized by cations released from the fallen litter, soil acidification would be mainly caused by excess cation accumulation in wood (3.0–8.6 $\text{kmol}_c\ \text{ha}^{-1}\ \text{year}^{-1}$) during forest growth.

Since protons react with silicate clay structure in the soils of Al buffering stages (soil pH < 5), Al in clay structures are solubilized. Assuming that most of acidity can be neutralized within the profiles, long-term acidification can be recorded as an increase in soil exchangeable Al^{3+}. When cumulative NPG_{Bio} attributable to

Fig. 7.8 Relationship between total NPG and ΔANC in the O horizons containing high or low concentrations of BC (basic cation). Data sources include five sites in Indonesia and one site in Thailand from the present study and three sites in Japan (1. Andisol, 2. Spodosol, 3. Inceptisol) from Fujii et al. (2008)

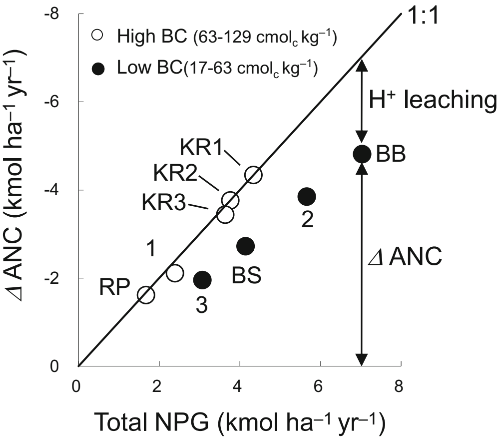

Fig. 7.9 Relationship between cumulative NPGBio attributable to wood production and exchangeable Al in the soils (0–30 cm). Data sources include five sites in Indonesia and one site in Thailand from the present study and three sites in Japan (1. Andisol, 2. Spodosol, 3. Inceptisol) from Fujii et al. (2008)

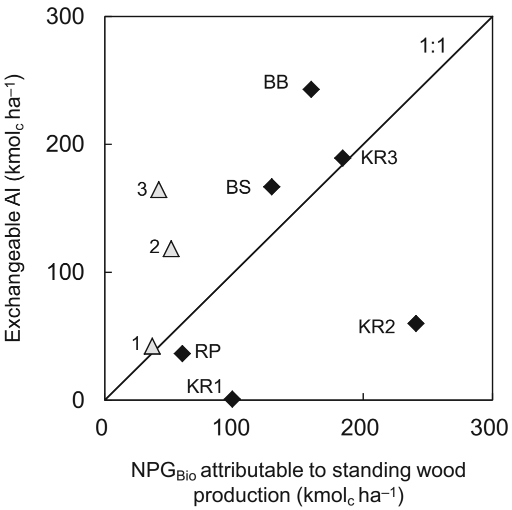

standing wood production and exchangeable Al^{3+} are compared, the amounts of soil exchangeable Al^{3+} are comparable to NPG_{Bio} attributable to wood production (Fig. 7.9). This also supports high contribution of plants to soil acidification. The exchangeable Al^{3+} was smaller than NPG_{Bio} in the KR1 and KR2 soils derived from serpentine and mudstone. This indicates buffering capacities of these soils are derived from the greater amounts of primary minerals as well as weathering of silicate minerals (Table 7.3). Our data support the idea that higher rates of cation cycling in plant-soil system result in consistently high acid loads to soils under tropical forest (Figs. 7.6 and 7.7).

7.4.2 Factors Regulating Proton Generation and Consumption in Soil Profiles

The dynamics of protons within the soil profiles can be quantified by application of proton budgets to each of soil horizons (Fig. 7.6). In all the soil profiles, the contribution of NPG_{Ntr}, NPG_{Car}, and NPG_{Org} to acidification is minor (Fig. 7.7). This is consistent with the fact that complete cycles of C and N are balanced with no net proton fluxes in forest ecosystems (Binkley 1987). However, translocation of the temporary acids (carbonic and organic acids and nitric acids), as well as distribution of fine root biomass (Fig. 7.3), contributes to heterogeneity of proton generation and consumption throughout the soil profiles, which varied from soil to soil, depending on geology and climate (Fig. 7.7).

Organic acid dissociation is a common proton-generating process in the O horizons of the forest soils studied. DOM-associated proton generation accounts for 18–77 % of total proton generation in the O horizons (Fig. 7.7). The large contribution of organic acids to acidification in the KR1, BS, and BB soils arises from the substantial fluxes of DOM production in the O horizon. This is primarily caused by the greater fluxes of precipitation and C input and quality of the foliar litter (Fujii et al. 2009b), as discussed in the following section.

On the other hand, carbonic acid dissociation is also a proton-generating process in the less acidic O horizons of the KR1 and KR2 soils (Table 7.5; $5 < \text{pH}$) because of their weakly acidic nature. Although NPG_{Car} is negligible in RP, bicarbonate can be a dominant anion in soil solution. This is consistent with substantial proton generation by carbonic acid dissociation in soils at neutral pH reported by Johnson et al. (1983), Van Breemen et al. (1984), and Gower et al. (1995). Although NPG_{Car} associated with active root and microbial respiration has generally been recognized as a dominant soil-acidifying process in tropical regions, the process is dominant only in moderately acidic and neutral soils.

Proton generation by nitrification is generally the dominant process involved in NPG_{Ntr} in the O horizons, while proton consumption by mineralization of organic N to NH_4^+ is also involved in NPG_{Ntr} in the highly acidic O horizons of the BS and BB soils (Figs. 7.5 and 7.7). These differences are dependent on the balance between mineralization, nitrification, and NH_4^+ and NO_3^- uptake by plants and microorganisms (Fig. 7.3). The rates of N mineralization by microorganisms are generally dependent on C/N ratio of substrates or soil environments and pH (Booth et al. 2005). Judging from most of the tropical soils and litters studied exhibiting relatively narrow C/N ratios, it was considered that ammonification is not a limiting step. Nitrification can be retarded by acidic conditions, as shown in NH_4^+ leaching from the highly acidic O horizons of the KR3, BS, and BB soils (Fig. 7.5).

NPG_{Bio} is the dominant proton-generating process in the mineral soil horizons of the KR1 and KR2 soils, while NPG_{Bio} is present in the O horizons of the KR3, BS, and BB soils (Figs. 7.3 and 7.7). Soil acidity and vegetation types could be the factors controlling the distribution of fine roots and thus NPG_{Bio}. In acidic soils, a fine root and ectomycorrhizal system is developed in the O horizon (Fujimaki et al.

2004). Dipterocarpaceae, which is the dominant vegetation on the BS and BB soils, has fine roots and ectomycorrhizal systems developed in the O horizons of acidic Ultisols (Ashton 1988). The high NPG_{Bio} in the O horizons of the KR3, BS, and BB soils arises from the presence of a fine root mat (0.3–2.3 Mg C ha^{-1} $year^{-1}$; Table 7.3), which is related to soil acidity ($pH < 4.5$) and ectomycorrhizal associations of Dipterocarpaceae in the BS and BB soils. Soil acidity and vegetation have a strong influence on the intensity and distribution of acids.

Release of cationic components is the principal mechanism of acid neutralization in organic and mineral soil horizons (Van Breemen et al. 1984). In the O horizons, the extent of acid neutralization varies with basic cation contents. The higher concentrations of basic cations in the O horizons of the KR soils (87–129 $cmol_c$ kg^{-1}) are considered to result in complete acid neutralization (Fig. 7.8). In the O horizons of the BS and BB soils, lower basic cation concentrations (17–63 $cmol_c$ kg^{-1}), as well as the intensive acid load, could result in incomplete acid neutralization and net eluviation of protons, Al, and Fe (Fig. 7.8).

In mineral soil horizons, the extents of acid neutralization depend on ANC of soils and their parent materials. Based on both published data and those from our study, soil ANC is variable, depending on parent materials and the extent of soil acidification or weathering and clay migration (Fig. 7.10). Our data show that parent materials have a strong influence on soil ANC with the BS and BB soils from sandstone having less ANC and a lower pH than the KR soils from serpentine and mudstone (Fig. 7.10). In the KR soils from serpentine or mudstone, their high ANC suggests that their acidity is completely neutralized by basic cation release (Figs. 7.8 and 7.10). In the BS and BB soils from sandstone, acidity is not completely neutralized due to their low ANC (Figs. 7.8 and 7.10). Thus, parent materials have a strong influence on acid neutralization processes through their effects on basic cation contents in the O horizons and on soil ANC.

7.4.3 *Significance of Dissolved Organic Matter Flux in Acidification and Nutrient Cycling in Tropical Forests of Southeast Asia*

Dissolved organic matter plays roles in cation mobilization and soil acidification (Guggenberger and Zech 1994). In forest soils, DOM is an intermediate by-product of litter decomposition by microorganisms (Guggenberger and Zech 1994). The formation of thick O horizons has typically been considered to lead to a sizable production of DOM in cool and humid climates (Michalzik et al. 2001). In tropical forests, the rapid mineralization of litter to CO_2 has been hypothesized to result in low concentrations of DOM in soil solutions (Johnson 1977). However, in the KR1, BS, and BB sites, a large flux of DOM is produced from the thin O horizon (Fig. 7.2; Fujii et al. 2009b, 2011c).

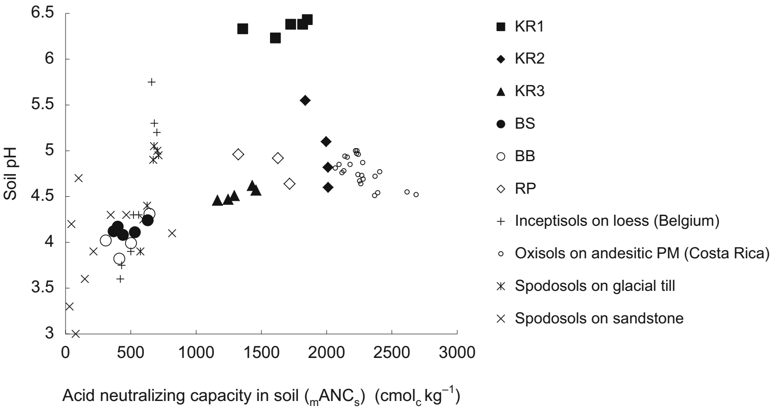

Fig. 7.10 Relationship between soil pH and acid-neutralizing capacity of soil ($_m$ANC$_s$). The data sources include Andriesse (1969) and Kleber et al. (2007). PM represents parent materials

Data synthesis indicated that large DOC fluxes from the O horizons in tropical forests can be caused by high precipitation and C input (sum of throughfall and litterfall) (Michalzik et al. 2001; Fujii et al. 2009b). The proportion of DOC flux relative to C input increased with decreasing pH (Fig. 7.11a), suggesting that the sizable production of DOC in the O horizons is common to acidic soils ($pH < 4.3$) in both temperate and tropical forests (Fujii et al. 2009b). The dominant DOM fractions leached from the O horizons are recalcitrant high-molecular-weight humic substances (Guggenberger and Zech 1994; Qualls and Bridgham 2005). The larger DOC flux at lower pH was considered to result from the release of aromatic compounds via lignin solubilization (Guggenberger and Zech 1993; Fujii et al. 2011b). Lignin solubilization is enhanced by the high activity of fungal enzymes [e.g., lignin peroxidase, Mn peroxidase; Fujii et al. (2012)], which contrasts with low microbial activity of cellulose degradation in the acidic soils (Hayakawa et al. 2014).

The DOC fluxes in the O horizon of KR1 were high despite high soil pH (Fig. 7.2), and this is an exceptional case of DOC flux-pH relationship (Fig. 7.11a). Within the five tropical forests in East Kalimantan, the magnitude of DOC leaching from the O horizons increased with decreasing P concentrations in the foliar litters (Fig. 7.11b; Fujii et al. 2011c). Low P concentrations in the foliar litter, as well as a high lignin concentration, could reduce DOC biodegradability and increase DOC leaching from the O horizons (Wieder et al. 2008). P concentrations in the foliar litter can account for DOC flux at local scale.

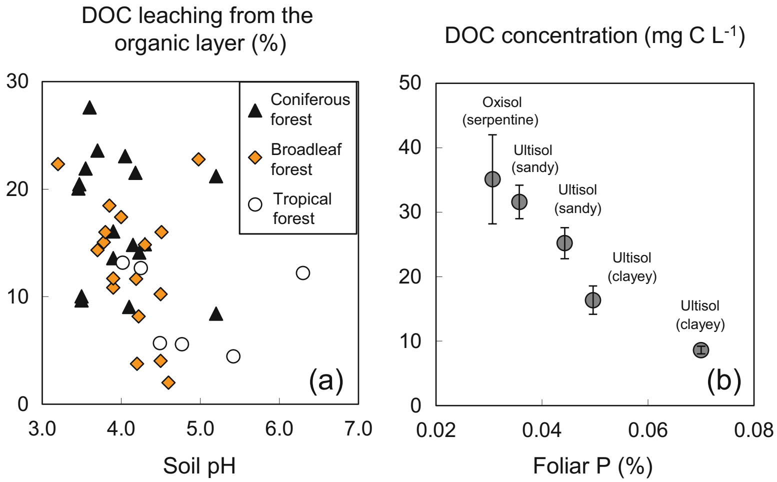

Fig. 7.11 Relationships between soil pH and DOC leaching from the O horizons (**a**) and foliar P concentrations and DOC concentrations in the O horizon leachate in five Indonesian forests (**b**). The DOC leaching was calculated as the proportion of DOC flux from the O horizons relative to C input (throughfall DOC and litterfall C). Data sources are Fujii et al. (2009b, 2011c)

7.4.4 *Implication of Proton Budgets for Pedogenetic Acidification*

The acid load is consistently higher in tropical regions than in temperate regions (Fig. 7.3). This supports the presence of strongly weathered soils in the humid tropics from the viewpoint of acidification (Eyre 1963). The kind, intensity, and distribution of acid load could vary with parent materials and vegetation, and therefore, weathering reactions and pedogenesis could also differ among tropical soils. The effects of parent materials on the dominant acidifying processes and pedogenesis can be characterized using the fluxes of Si, Al, and Fe and proton budgets within the soil profiles (Table 7.8; Fig. 7.7).

Judging from the low concentrations of Al and Fe in the moderately acidic and neutral soil solutions of the KR1 and KR2 soils (Table 7.7), the accumulated Al and Fe oxides appear to arise from in situ weathering rather than eluviation/illuviation processes. In the KR1 soil, the substantial fluxes of Si (2.67–3.55 kmol ha^{-1} year^{-1} from Table 7.8) and the high contents of Fe oxides throughout the soil profiles (Table 7.4) support the concept of ferralitization, which implies an absolute loss of Si (c) and a relative accumulation of Al and Fe oxides (Cornu et al. 1998). Dissolution of olivine by acids [$Mg_{1.6}Fe_{0.4}SiO_4$ (olivine) + $4H^+ = 1.6\ Mg^{2+} + 0.4Fe^{2+} + H_4SiO_4$] and Si leaching are considered to result in desilication, shown by a decrease of Si content from 45 % for serpentine to 9 % in the KR1 soil (Effendi et al. 2000). The fluxes of Si leaching from the KR1 soil (3.55 kmol Si ha^{-1} year^{-1}) are higher than those of Oxisols from sedimentary rocks under Amazonian forests (1.1 kmol Si ha^{-1} year^{-1}) because of the higher dissolution rates of serpentine (olivine) than quartz and kaolinite (Cornu et al. 1998). This is consistent with the rapid formation of Oxisols (ferralitization) from easily weatherable serpentine, as compared to sedimentary rocks (Pfisterer et al. 1996).

In the KR2 and KR3 soils from sedimentary rocks, no net loss of Si occurs. In the KR2 soil, the high rates of NPG_{Car} and minor contribution of NPG_{Org} to soil acidification have contributed to incongruent dissolution of Fe-rich parent materials, which results in accumulation of Al and Fe oxides throughout the profile. This process in the KR2 soil is similar to brunification, which implies accumulation of Al and Fe oxides owing to incongruent dissolution by weak acids (e.g., carbonic acid) in brown forest soils formed under temperate forest (Ugolini et al. 1990; Fujii et al. 2008).

In the highly acidic BS and BB soils, the intensive acid load contributed by NPG_{Org} and NPG_{Bio} in the O horizons results in net eluviation of protons, Al, and Fe (Fig. 7.7). These acidification processes are similar to podzolization (Cronan and Aiken 1985; Guggenberger and Kaiser 1998; Fujii et al. 2008), which involves the complexing of Al and Fe with organic acids and their translocation downward. However, translocation of Al and Fe in the BS and BB soils is different from podzolization because of the absence of spodic B horizons. The degree of podzolization is considered to be controlled by the ANC and Fe contents in the parent materials (Duchaufour and Souchier 1978; Do Nascimento et al. 2008). The higher ANC and Fe content in the BS and BB soils (Table 7.4; 309–643 $\text{cmol}_c\ \text{kg}^{-1}$ and 3.6–3.9 $\%\text{Fe}_2\text{O}_3$, respectively), as compared to the typical values for the tropical Spodosols (av. 291 $\text{cmol}_c\ \text{kg}^{-1}$ and $< 2\ \%\text{Fe}_2\text{O}_3$, respectively; Fig. 7.11), is considered to reduce the mobility of organic acids and the degree of podzolization.

7.4.5 *Ecological Significance of Soil Acidification in Tropical Forests*

Proton budgets showed that there are similarities and dissimilarities in soil acidification patterns between tropical forests. The similarity of soil acidification processes between tropical forests is high cation demand by plants. Plants can take up the large amounts of basic cations mobilized through acidification (Fig. 7.6). This leads to a decrease in ANC in most of the soils, but buffering mechanisms are different between parent materials (Fig. 7.10). Acidification leads to accumulation of exchangeable Al in the highly acidic Ultisol soils on sandstone, while it leads to loss of basic cations in the soils on mafic parent materials (Fig. 7.9).

One of dissimilarities in soil acidification processes between tropical forest soils is flux of DOM (or organic acids) from the O horizon. Organic acids are well known to play roles in Al detoxification and P solubilization (Jones 1998). The high concentrations of DOM might be responses of plants and microorganisms to high Al toxicity in the highly acidic Ultisols containing the high concentrations of exchangeable Al and soil solution Al ions (Tables 7.4 and 7.7).

In addition, DOM can transport N and P in organic form (Qualls et al. 1991). The proportions of DON to TDN in the O horizon solutions (13–40 %) are smaller than temperate coniferous forests (Table 7.8; Fig. 7.4). These values are within the range of tropical forests and temperate broad-leaved forests exhibiting narrow CN ratio of the foliar litters (Fuji et al. 2013).

Because DOM leached from the O horizons is stabilized by sorption onto clays in the mineral soil horizons, leaching loss from the soil is minimal (Fig. 7.6). Once DOM is stabilized in the mineral horizons, soil organic matter functions as a reservoir and slow-release source of N, P, and bases (Kalbitz et al. 2000). The production of tannin-rich litter is hypothesized to be an adaptive strategy of coniferous trees for minimizing the leaching loss of N from nutrient-limited forests (Northup et al. 1995a, b). In the P-limited tropical forests of Southeast Asia, DOM can increase P solubility in the surface soil through the competition for sorption sites by organic anions and can minimize loss of dissolved organic P through sorption in the subsoil (Fig. 7.11 b).

There might exist two different mechanisms of acidification that drive tight nutrient cycling in tropical forests. Tropical forests in Central America develop efficient nutrient cycles through carbonic acid leaching in the moderately acidic soils (Johnson 1977). The soil acidification process in the moderately acidic soils derived from mafic parent materials (high ANC) in our study are close to this pattern. On the other hand, tropical forests on sedimentary rocks (low ANC) appear to develop DOM (or organic acid)-driven nutrient cycling on the highly acidic soils to acquire bases and P and minimize their losses.

7.5 Conclusions

The proton budgets in the soils showed quantitatively that soil acidification is an ongoing process in tropical forests due to high primary productivity. The dominant soil-acidifying process is excessive accumulation of cations over anions in woody biomass. This finding is common in a variety of the soils under tropical forests. Although soil acidification has typically been recognized as one of land degradation, acidification by plants and microorganisms can be one of nutrient acquisition strategies that promote cation mobilization through mineral weathering and cation exchange reaction. When proton generation and consumption were analyzed for each of soil horizons, proton-generating processes are variable depending ANC of parent materials even within tropical forests. In the O horizons of the highly acidic soils, dissociation of organic acids and plant uptake contributed to intensive acidification of surface horizons. In the less acidic soils, production of carbonic acid (bicarbonate) and nitric acid can contribute to leaching of cations. In the mineral soil horizons, protons generated by plant uptake are consumed by mineralization and sorption of organic acids, nitrate uptake by plants, and basic cation or Al/Fe release from the soil. The spatiotemporal variation in roots and acids can cause different pathways of pedogenesis, incipient podzolization (Al eluviation/

illuviation) and ferralitization (in situ weathering). The production of DOM, the sources of organic acids, can be enhanced by the lignin-rich and P-poor foliar and woody litters and the high activities of fungal enzymes (peroxidases) in the highly acidic soils. The differences in acid-neutralizing capacities of parent materials and climatic patterns can generate the variability in soil acidity, and plant and microbial feedbacks can further reinforce the patterns of soil acidification and nutrient cycling. Understanding of soil acidification mechanisms in different geological and climatic conditions is helpful to minimize the potential impacts of land use changes (conversion of forests to agricultural lands) on soil fertility or to accelerate restoration of the ecosystems damaged by human disturbances (e.g., fires).

References

Andriesse JP (1969) A study of the environment and characteristics of tropical podzols in Sarawak (East-Malaysia). Geoderma 2:201–227

Ashton PS (1988) Dipterocarp biology as a window to the understanding of tropical forest structure. Annu Rev Ecol Syst 19:347–370

Binkley D (1992) Proton budgets. In: Johnson DW, Lindberg SE (eds) Atmospheric deposition and forest nutrient cycling. Ecol Stud 91:450–466, Springer, New York

Binkley D, Richter D (1987) Nutrient cycles and H+ budgets of forest ecosystems. Adv Ecol Res 16:2–51

Booth MS, John MS, Edward R (2005) Controls on nitrogen cycling in terrestrial ecosystems: a synthetic analysis of literature data. Ecol Monogr 75:139–157

Brahy V, Deckers J, Delvaux B (2000) Estimation of soil weathering stage and acid neutralizing capacity in a toposequence Luvisol-Cambisol on loess under deciduous forest in Belgium. Eur J Soil Sci 51:1–13

Bredemeier M, Matzner E, Ulrich B (1990) Internal and external proton load to forest soils in Northern Germany. J Environ Qual 19:469–477

Busman LM, Dick BP, Tabatabai MA (1983) Determination of total sulfur and chlorine in plant materials by ion chromatography. Soil Sci Soc Am J 47:1167–1170

Connell J, Lowman MD (1989) Low-diversity tropical rain forests: some possible mechanisms for their existence. Am Nat 134:88–119

Cornu S, Lucas Y, Ambrosi JP, Desjardins T (1998) Transfer of dissolved Al, Fe and Si in two Amaznian forest environments in Brazil. Eur J Soil Sci 49:377–384

Cronan CS, Aiken GR (1985) Chemistry and transport of soluble humic substances in forested watersheds of the Adirondack park, New York. Geochim Cosmochim Acta 49:1697–1705

Do Nascimento NR, Fritsch E, Bueno GT, Bardy M, Grimaldi C, Melfi AJ (2008) Podzolization as a deferralitization process: dynamics and chemistry of ground and surface waters in an Acrisol-Podzol sequence of the upper Amazon Basin. Eur J Soil Sci 59:911–924

Duchaufour P, Souchier B (1978) Roles of iron and clay in genesis of acid soils under a humid, temperate climate. Geoderma 20:15–26

Effendi S, Miura S, Tanaka N, Ohta S (2000) Serpentine soils on catena in the southern part of East Kalimantan, Indonesia. In: Guhardja E, Fatawi M, Sutisna M, Mori T, Ohta S (eds) Rainforest ecosystems of East Kalimantan, Ecological studies, vol 140. Springer, Tokyo

Eyre SR (1963) Vegetation and Soils: a world picture. Edward Arnold, London

Fujii K (2014) Soil acidification and adaptations of plants and microorganisms in Bornean tropical forests. Ecol Res 29:371–381

Fujii K, Funakawa S, Hayakawa C, Kosaki T (2008) Contribution of different proton sources to pedogenetic soil acidification in forested ecosystems in Japan. Geoderma 144:478–490

Fujii K, Funakawa S, Hayakawa C, Sukartiningsih FS, Kosaki T (2009a) Quantification of proton budgets in soils of cropland and adjacent forest in Thailand and Indonesia. Plant Soil 316:241–255

Fujii K, Uemura M, Funakawa S, Hayakawa C, Sukartiningsih FS, Kosaki T, Ohta S (2009b) Fluxes of dissolved organic carbon in two tropical forest ecosystems of East Kalimantan, Indonesia. Geoderma 152:127–136

Fujii K, Hartono A, Funakawa S, Uemura M, Sukartiningsih FS, Kosaki T (2011a) Distribution of Ultisols and Oxisols in the serpentine areas of East Kalimantan, Indonesia. Pedologist 55:63–76

Fujii K, Funakawa S, Shinjo H, Hayakawa C, Mori K, Kosaki T (2011b) Fluxes of dissolved organic carbon and nitrogen throughout andisol, spodosol and inceptisol profiles under forest in Japan. Soil Sci Plant Nutr 57:855–866

Fujii K, Hartono A, Funakawa S, Uemura M, Kosaki T (2011c) Fluxes of dissolved organic carbon in three tropical secondary forests developed on serpentine and mudstone. Geoderma 163:119–126

Fujii K, Uemura M, Hayakawa C, Funakawa S, Kosaki T (2012) Environmental control of lignin peroxidase, manganese peroxidase, and laccase activities in forest floor layers in humid Asia. Soil Biol Biochem 57:109–115

Fujii K, Hayakawa C, Funakawa S, Sukartiningsih FS, Kosaki T (2013) Fluxes of dissolved organic carbon and nitrogen in cropland and adjacent forest in a clay-rich Ultisol of Thailand and a sandy Ultisol of Indonesia. Soil Tillage Res 126:267–275

Fujimaki R, Tateno R, Hirobe M, Tokuchi N, Takeda H (2004) Fine root mass in relation to soil N supply in a cool temperate forest. Ecol Res 19:559–562

Gower C, Rowell DL, Nortcliff S, Wild A (1995) Soil acidification: comparison of acid deposition from the atmosphere with inputs from the litter/soil organic layer. Geoderma 66:85–98

Guggenberger G, Kaiser K (1998) Significance of DOM in the translocation of cations and acidity in acid forest soils. Zeitschrift für Pflanzenernährung, Düngung und Bodenkunde 161:95–99

Guggenberger G, Zech W (1993) Dissolved organic carbon control in acid forest soils of the Fichtelgebirge (Germany) as revealed by distribution patterns and structural composition analyses. Geoderma 59:109–129

Guggenberger G, Zech W (1994) Dissolved organic carbon control in forest floor leachate: simple degradation products or humic substances? Sci Total Environ 152:37–47

Hallbäcken L, Tamm CO (1986) Changes in soil acidity from 1927 to 1982–1984 in a forest area of south-west Sweden. Scand J For Res 1:219–232

Hayakawa C, Funakawa S, Fujii K, Kadono A, Kosaki T (2014) Effects of climatic and soil properties on cellulose decomposition rates in temperate and tropical forests. Biol Fertil Soils 50:633–643

Jackson ML (1958) Soil chemical analysis. Prentice-Hall, Inc., Englewood Cliffs

Johnson DW (1977) Carbonic acid leaching in a tropical temperate, subalpine, and northern forest soil. Arct Alp Res 9(4):329–343

Johnson FL, Risser PG (1974) Biomass, annual net primary production, and dynamics of six mineral elements in a post oak-blackjack oak forest. Ecology 55:1246–1258

Johnson DW, Richter DD, Van Miegroet H, Cole DW (1983) Contributions of acid deposition and natural processes to cation leaching from forest soils: a review. J Air Pollut Control Assoc 33:1036–1041

Jones DL (1998) Organic acids in the rhizosphere—a critical review. Plant Soil 205:25–44

Kalbitz K, Solinger S, Park JH, Michalzik B, Matzner E (2000) Controls on the dynamics of dissolved organic matter in soils: a review. Soil Sci 165:277–304

Kleber M, Schwendenmann L, Veldkamp E, Rößner J, Jahn R (2007) Halloysite versus gibbsite: silicon cycling as a pedogenetic process in two lowland neotropical rain forests soils of La Selva, Costa Rica. Geoderma 138:1–11

Klinge R (2001) Simulation of water drainage of a rain forest and forest conversion plots using a soil water model. J Hydrol 246:82–95

Krug EC, Frink CR (1983) Acid rain on acid soil: a new perspective. Science 221:520–525

McDowell WH (1998) Internal nutrient fluxes in a Puerto Rican rain forest. J Trop Ecol 14:521–536

Mehra OP, Jackson ML (1960) Iron oxide removal from soils and clays by a dithionite-citrate system buffered with sodium bicarbonate. Clay Clay Miner 7:317–327

Michalzik B, Kalbitz K, Park JH, Solinger S, Matzner E (2001) Fluxes and concentrations of dissolved organic carbon and nitrogen—a synthesis for temperate forests. Biogeochemistry 52:173–205

Mualem Y, Dagan G (1978) Hydraulic conductivity of soils: unified approach to the statistical models. Soil Sci Soc Am J 42:392–395

Nakane K (1980) Comparative studies of cycling of soil organic carbon in three primeval moist forests. Jpn J Ecol 3:155–172

Northup RR, Dahlgren RA, Yu Z (1995a) Intraspecific variation of conifer phenolic concentration on a marine terrace soil acidity gradient: a new interpretation. Plant Soil 171:255–262

Northup RR, Yu Z, Dahlgren RA, Vogt KA (1995b) Polyphenol control of nitrogen release from pine litter. Nature 377:227–229

Pfisterer U, Blume HP, Kanig M (1996) Genesis and dynamics of an oxic dystrochrept and a typic haploperox from ultrabasic rock in the tropical rain forest climate of south-east Brazil. Z Pflanzenernährung Düng Bodenkd 159:41–50

Qualls RG, Bridgham SD (2005) Mineralization rate of ^{14}C-labeled dissolved organic matter from leaf litter in soils of a weathering chronosequence. Soil Biol Biochem 37:905–916

Qualls RG, Haines BL, Swank WT (1991) Fluxes of dissolved organic nutrients and humic substances in a deciduous forest. Ecology 72:254–266

Sanchez, P.A., Logan, T.J. 1992. Myths and science about the chemistry and fertility of soils in the tropics. In: Lal, R., Sanchez, P.A. (eds) Myths and science of soils in the tropics, SSSA Special Publication 29. ASA and SSSA, Madison, pp 35–46.

Shibata H, Kirikae M, Tanaka Y, Sakuma T, Hatano R (1998) Proton budgets of forest ecosystem on canogenous regosols in Hokkaido. Water Air Soil Pollut 105:63–72

Shibata H, Satoh F, Sasa K, Ozawa M, Usui M, Nagata O, Hayakawa Y, Hatano R (2001) Importance of internal proton production for the proton budget in Japanese forested ecosystems. Water Air Soil Pollut 130:685–690

Soil Survey Staff (2006) Keys to soil taxonomy, Tenth edn. United States Department of Agriculture Natural Resources Conservation Service, Washington, DC

Thurman, E.M., 1985. Humic substances in groundwater. In: Aiken, G.R., McKnight, D.M., Wershaw, R.L., MacCarthy, P. (Eds.), Humic substances in soil, sediment, and water. Wiley, New York, pp 87–103.

Ugolini FC, Sletten RS (1991) The role of proton donors in pedogenesis as revealed by soil solution studies. Soil Sci 151:59–75

Ugolini FC, Sletten RS, Marrett DJ (1990) Contemporary pedogenic processes in the artic: brunification. Sci du sol 28:333–348

Van Breemen N, Mulder J, Driscoll CT (1983) Acidification and alkalization of soils. Plant Soil 75:283–308

Van Breemen N, Driscoll CT, Mulder J (1984) Acidic deposition and internal proton in acidification of soils and waters. Nature 307:599–604

Van Genuchten MT (1980) A closed-form equation for predicting the hydraulic conductivity of unsaturated soils. Soil Sci Soc Am J 44:892–898

Vitousek PM, Howarth RW (1991) Nitrogen limitation on land and in the sea: how can it occur? Biogeochemistry 13:87–115

Wieder WR, Cleveland CC, Townsend AR (2008) Tropical tree species composition affects the oxidation of dissolved organic matter from litter. Biogeochemistry 88:127–138

Yamakura T, Hagihara A, Sukardjo S, Ogawa H (1986) Aboveground biomass of tropical rain forest stands in Indonesia Borneo. Vegetation 68:71–82